Available online at www.eccomasproceedia.org
Eccomas Proceedia COMPDYN (2025) 1889-1899

ECCOMAS

Proceedia

COMPDYN 2025
10th ECCOMAS Thematic Conference on
Computational Methods in Structural Dynamics and Earthquake Engineering
M. Papadrakakis, M. Fragiadakis (eds.)
Rhodes Island, Greece, 15-18 June 2025

DEFINITION OF A SIMPLIFIED DESIGN PROCEDURE FOR ENERGY DISSIPATION DEVICES COUPLED WITH SEISMIC ISOLATION SYSTEMS

Furinghetti M.[1,2]

[1] DICAr - Civil Engineering and Architecture Department
University of Pavia
via Ferrata 3, 27100 Pavia, Italy
e-mail: marco.furinghetti@unipv.it

[2] EUCENTRE Foundation
European Centre for Training and Research in Earthquake Engineering
via Ferrata 1, 27100 Pavia, Italy
email: marco.furinghetti@eucentre.it

Abstract

Seismic isolation represents a very effective strategy for the reduction of the structural vulnerability of buildings and bridges. The isolator technologies available in the common practice can easily lead to a significant limitation of the base shear of the system, with resulting lower internal forces for all structural members. Simultaneously, large displacement demands can be accommodated by isolators, even when the damping characteristics are not so relevant. However, depending on the size of the structure and on the seismic hazard of the construction site, the design of rubber bearing devices can lead to hybrid systems, and a number of flat sliders have to be adopted, and in some cases few isolators can be found. An increased number of isolators could be obtained, if additional energy dissipation devices are properly designed, in order to obtain a better definition of the isolation system. In this research work a simplified design procedure for energy dissipation devices is presented, when additional damping is needed for seismically isolated structural systems. Results of the presented procedure have been numerically validated through Non- Linear Time History Analyses, and the single-event and the mean responses have been compared to the target design values.

Keywords: Fluid Viscous Dampers, Seismic Isolation, Rubber Bearings, Non-Linear Time History Analyses, Fast Design Procedure.

doi: 10.7712/120125.12537.26114

1 INTRODUCTION

The presented research aims at providing a fast design procedure for seismic isolation systems, based on elastomeric bearings and fluid viscous dampers. Rubber isolators represent the easiest solution for seismic risk mitigation, with simple modeling assumptions and significant recentering behaviors ([1], [5], [9]). On the other hand a limited energy dissipation capacity is met, in comparison to other available technologies ([7] , [8] , [11] , [14] , [15]), and possible adoption of additional flat sliders is needed ([9]), in order to cover all the structural bearing points.
A detailed design procedure is presented, which allows to return both geometrical and mechanical characteristics of the isolation and energy dissipation devices. Through very few steps, practitioners and researchers are able to design the isolation system, by providing the proper protection to the superstructure, thanks to some simplifications which provide approximated results, significantly close to the exact solution. The proposed procedure has also been validated by means of Non-Linear Time History Analyses, performed on a case study structure.

2 CASE STUDY STRUCTURE

In Figure 1 the case study structure used to validate the proposed design procedure is shown.

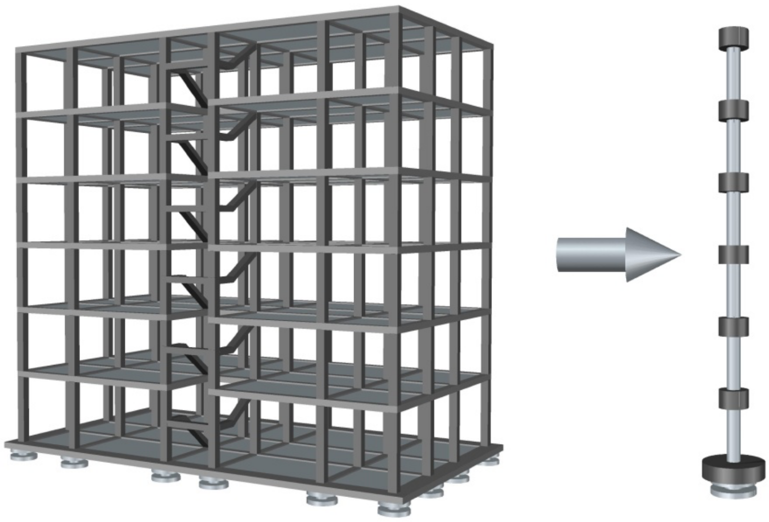

Figure 1: Case study structure.

The building consists of a 6 storey frame structure, with reinforced concrete beams and columns. The plan dimensions are approximately 20m along the x direction and 10m along the y direction, with a total height of 19m ([2]). The total mass of the whole structural system is equal to 2040ton: such a value has been used for the application of the proposed fast design procedure, described as follows.

3 FAST DESIGN PROCEDURE

The overall procedure have been defined through few steps, which are characterized by very simple assumptions ([12]). Initially, the considered case study structure is assumed to be characterized by a specific "Performance Point" for the isolation system, which is univocally determined by two important parameters:

- The Design Period T_d, in terms of secant period at maximum displacement.
- The Design Equivalent Viscous Damping of the isolation systems ξ_d, which is a function of the dissipation capability of the adopted devices.

The definition of such a performance point can be considered, since the overall base-isolated structural system can be approximated to a condensed equivalent Single Degree of Freedom (SDOF) oscillator and reasonable comparisons between the two systems can be found, even though the adopted devices are characterized by a non-linear and hysteretic force response. Generally, standard codes worldwide allow designers to model non-linear devices through linear modeling approaches under specific conditions, depending on the energy dissipation capacity and the force response characteristics of the devices ([3], [16]). Nonetheless, for initial design purposes, the behavior of an equivalent SDOF oscillator provides fairly good estimate of the global behavior of the base-isolated structure. Hence, given the seismic hazard of the considered construction site, in terms of displacement and acceleration response spectra, the performance point is univocally computed, as displacement demand and peak normalized force response respectively (normalized with respect to the total mass of the overall system).
Since a seismic isolation system based on Rubber Bearings and Fluid Viscous Dampers is considered in this work, the elastomeric isolators will be associated to a low stiffness level of the structure, able to lead to the proper period shift of the structure, whereas damping devices will be responsible of the whole energy dissipation capability. In other words, the total energy dissipation will be addressed to Fluid Viscous Dampers only, and the limited contribution related to the rubber compound characteristics will be neglected.
Similarly to the design procedure of purely elastomeric-based isolation systems, the first step is the computation of the height of the device h_{is}, thanks to the assumption of the design shear strain of the rubber isolator γ_d, which is generally considered equal to 100%. Thus, given the displacement demand D_d, represented by the spectral displacement $Sd(T_d,\xi_d)$ at the design period, by accounting for the design equivalent damping ratio:

$$h_{is} = \frac{Sd(T_d, \xi_d)}{\gamma_d} = \frac{D_d}{\gamma_d} \tag{1}$$

It has to be noted that the numerical value of the adopted equivalent viscous damping ratio is no longer addressed to the characteristics of the rubber compound (from 5% to 10% for LDRB and from 10% up to 15% for HDRB): since the energy dissipation is provided by ad hoc designed Fluid Viscous Dampers, a much larger Equivalent Viscous Damping ratio can be considered. More specifically, values bounded between 20% and 30% can be feasible, thus comparable to LRB and CSS isolation systems, which are characterized by significant hysteretic behaviors.
Consequently, for the computation of the horizontal sizes of the device, the diameter of the plan section Φ_r can be obtained by scaling the design displacement demand by a proper scale factor, in order to avoid buckling phenomena when the maximum shear strain is achieved, and to guarantee the proper vertical bearing capacity of the devices; numerical simulations have shown that a multiplication factor equal to 2.0 generally leads to correct definitions of both the shape factors S1 and S2 [2]. Therefore, the following equation is obtained:

$$\Phi_r \approx 2 \cdot D_d \tag{2}$$

Once the geometrical characteristics of the elastomeric isolators have been computed, the lateral stiffness of the single device k_{is} can be computed, by considering that all the bearing points of the system are provided with elastomeric isolators: consequently, the single-device stiffness is equal to the ratio between the global isolation stiffness and the number of bearing points. Then, the shear modulus G_r of the elastomeric compound can be computed, as a function of the bearing's sizes (height h_{is} and rubber area section A_r) and the single-device stiffness.

$$k_{is} = \frac{G_r \cdot A_r}{h_{is}} = \frac{K_{esi}}{n_{is}} \tag{3}$$

$$G_r = \frac{K_{esi} \cdot h_{is}}{A_r \cdot n_{is}} \tag{4}$$

Thus, since the energy dissipation has to be addressed to Fluid Viscous Damper devices only, the analytical expression of the Energy Dissipated per Cycle (EDC) has to be obtained, by considering a fully reversed symmetric cycle *C*, as ruled by the Jacobsen's formulation of the equivalent viscous damping. To this aim, a sinusoidal displacement time series is considered, with a given frequency value *f*. Consequently, the expressions of the velocity and the Fluid Viscous Dampers force response time series can be obtained.

$$D(t) = D_d \cdot \sin(2\pi f t) \tag{5}$$

$$V(t) = 2\pi f D_d \cdot \cos(2\pi f t) = V_d \cdot \cos(2\pi f t) \tag{6}$$

$$F_{FVD}(t) = sign\big(V(t)\big) \cdot C \cdot |V(t)|^\alpha \tag{7}$$

Hence, the Energy Dissipated per Cycle can be computed as the integral of the force-displacement hysteretic loop, related to the Fluid Viscous Dampers only. Then, since the hysteretic shape of the loop is symmetric along both the horizontal and vertical axes, the expression can be simplified by considering four times the force-displacement integral of a quarter of cycle *C/4*. Then, the integral can be expressed within the time domain, as reported in Eq(10).

$$EDC = \int_C F_{FVD} \cdot du_0 = \int_C sign\big(V(t)\big) \cdot C \cdot |V(t)|^\alpha \cdot du_0 \tag{8}$$

$$EDC = 4 \cdot \int_{C/4} C \cdot V(t)^\alpha \cdot du_0 = 4 \cdot \int_{C/4} C \cdot V(t)^\alpha \cdot 2\pi f D_d \cdot \cos(2\pi f t) \cdot dt \tag{9}$$

$$EDC = 4 \cdot \int_{0}^{1/4f} C \cdot V_d^{\alpha} \cdot \cos^{\alpha}(2\pi f t) \cdot V_d \cdot \cos(2\pi f t) \cdot dt \tag{10}$$

In order to consider a dimensionless parameter, for an easier formulation, the EDC expression has been divided by the maximum displacement of the cycle and the peak design force of the whole set of Fluid Viscous Dampers. Thus, a normalized Energy ε_{FVD} has been obtained.

$$\varepsilon_{FVD} = \frac{EDC}{D_d \cdot C \cdot V_d^{\alpha}} = 8\pi f \cdot \int_{0}^{1/4f} \cos^{\alpha+1}(2\pi f t) \cdot dt \tag{11}$$

The last equation can be solved numerically, by varying the numerical value of the velocity exponent α, which is a design parameter to be assumed, by considering the available technology of damping devices. It has to be noted that α assumed values between 0.0 and 1.0, since Fluid Viscous Dampers are considered in this study (for values higher than 1.0 devices behave as Shock Transmission Units - STU). In Figure 2 numerical results of the aforementioned integral are shown. Numerical simulations have shown that the normalized energy is not affected by the numerical value of the frequency of motion.

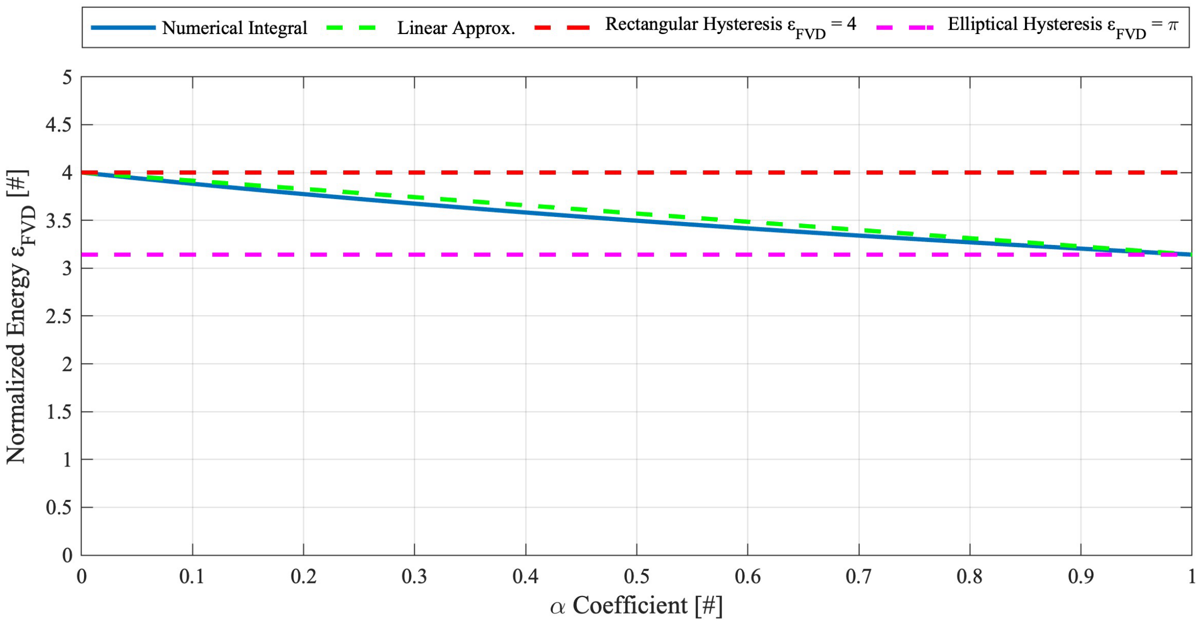

Figure 2: Dependency of the Normalized Energy on the Velocity Exponent.

The graphical trend of the numerical integral shows an approximately linear behavior between the normalized energy and the velocity exponent. In addition, the starting and ending values of the graph represent specific configurations: namely, $\alpha = 0$ represents a pure frictional behavior, characterized by a rectangular hysteresis shape; on the other hand, $\alpha = 1$ represents an ideal linear dashpot, characterized by an elliptical hysteresis shape, as shown in Figure 3.

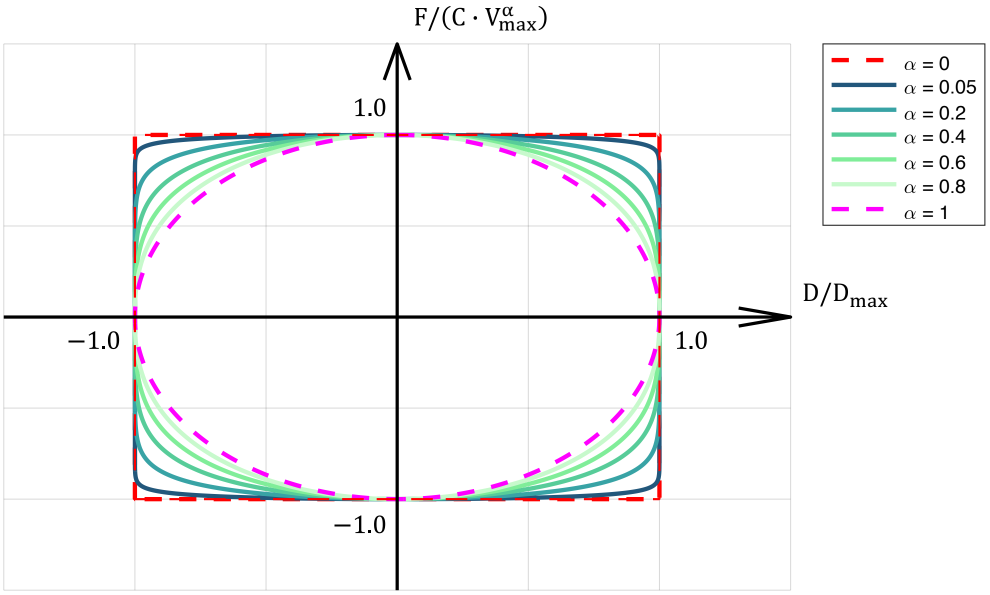

Figure 3: Dependency of the Hysteretic Shape Variability on the Velocity Exponent.

Consequently, the correspondent values of normalized energy at the boundaries of the considered velocity exponent range, $\varepsilon_{FVD} = 4$ and $\varepsilon_{FVD} = \pi$, respectively for $\alpha = 0$ and $\alpha = 1$. Thus, if an approximated linear trend is considered for the normalized energy, the following expression can be obtained for the Energy Dissipated per Cycle:

$$EDC = \varepsilon_{FVD} \cdot D_d \cdot C \cdot V_d^{\alpha} \approx [4 - \alpha \cdot (4 - \pi)] \cdot D_d \cdot C \cdot V_d^{\alpha} \tag{12}$$

At this stage, the final aim is represented by the computation of the total damping coefficient, which has to be equally smeared on the implemented Fluid Viscous Dampers. To do so, the expression of the EDC is substituted within the Jacobsen's formulation of the equivalent viscous damping ratio, as follows:

$$\xi_d = \frac{EDC}{2\pi \cdot D_d \cdot F_{max}} = \frac{\varepsilon_{FVD} \cdot D_d \cdot C \cdot V_d^{\alpha}}{2\pi \cdot D_d \cdot F_{max}} = \frac{\varepsilon_{FVD} \cdot C \cdot V_d^{\alpha}}{2\pi \cdot F_{max}} \tag{13}$$

Being the maximum force the peak force response of all the elastomeric isolators (in terms of product between the global stiffness and the design displacement), the total damping coefficient of the whole set of Fluid Viscous Dampers can be obtained, as a function of the initially assumed equivalent viscous damping ratio.

$$C = \frac{2\pi \cdot F_{max} \cdot \xi_d}{\varepsilon_{FVD} \cdot V_d^{\alpha}} \tag{14}$$

Finally, such a parameter can be equally divided by the number of Fluid Viscous Dampers, in order to obtain the single-device damping coefficient c_{FVD}.

4 DYNAMIC SYSTEM AND SEISMIC INPUT

The proposed design procedure has been applied to the case study structure, by considering the seismic hazard of L'Aquila city in Italy, correspondent to Collapse Limit State (5% probability of exceedance in 50 years, with a resulting return period of 975 years) soil classification C and topographic category T1. Results have been compared to the outcomes of Non-Linear Time History Analyses, performed by applying a suite of seven spectrum compatible ground motion time series ([13]), as shown in Figure 4.

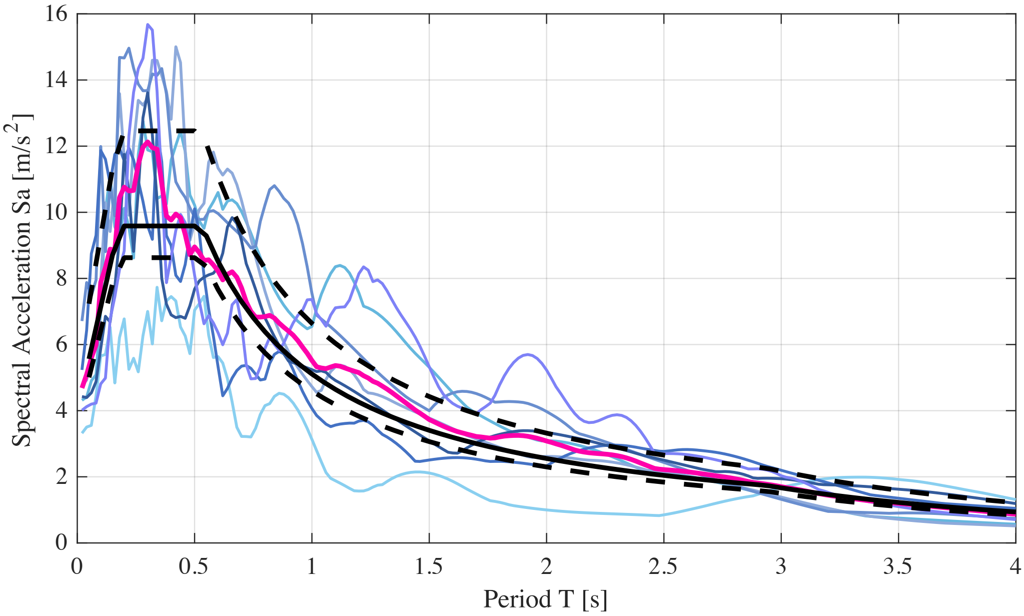

Figure 4: Spectrum Compatibility of the selected Ground Motion recordings.

In Table 1 and Table 2 the obtained design parameters are summarized for both elastomeric isolators and fluid viscous dampers.

Table 1. Characteristics of the designed elastomeric isolators

$T_d\ [s]$	ξ_d [%]	$D_d\ [m]$	γ_d [%]	$h_{is}\ [mm]$	$\Phi_r\ [mm]$	$G_r\ [MPa]$
3.5	27.6	0.210	100	210	421	0.4

Table 2. Characteristics of the designed damping devices

$V_d\ [mm/s]$	α [#]	$C\ [kNs^\alpha/m^\alpha]$	n_{FVD} [#]	$C_{FVD}\ [kNs^\alpha/m^\alpha]$
0.378	0.4	967.4	4	241.9

In order to perform NLTHA, the full 3D finite element model of the structural system has been statically condensed into a Multi Degree of Freedom oscillator, characterized by the same dynamic properties, in terms of modal shapes and vibration period values for the fixed-base configuration, by implementing the proper non-linear hysteretic force response at the isolation level ([6]).

5 RESULTS

In what follows results of the NLTHA are presented, for both the single-event and the mean responses. More specifically, special attention has been focused on the peak isolation displacement and velocity (Figure 5 and Figure 5), the building base shear (Figure 7) and the building interstorey drift (Figure 8).

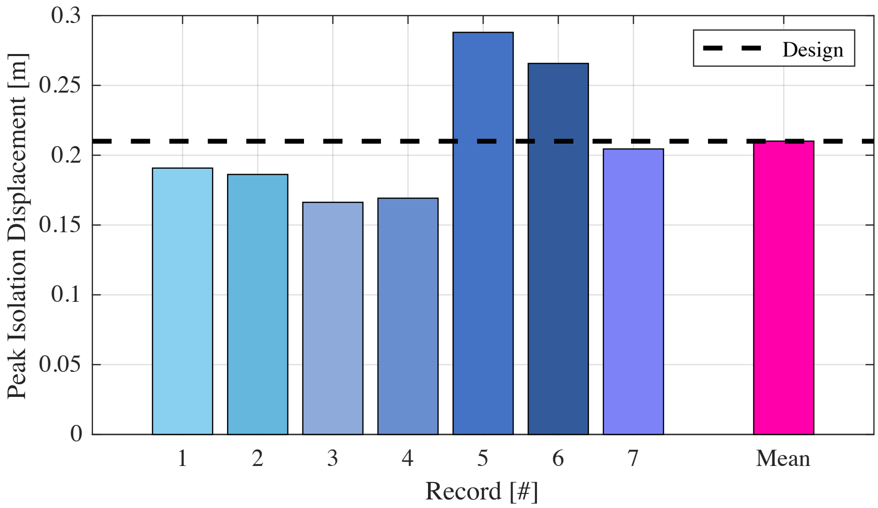

Figure 5: Results: peak isolation displacement.

Displacement results show that the proposed design procedure for isolation systems equipped with elastomeric bearings and fluid viscous dampers provides a good solution for the evaluation of the mechanical and geometrical properties of the devices, not only for the average response, but also for the single-event cases.

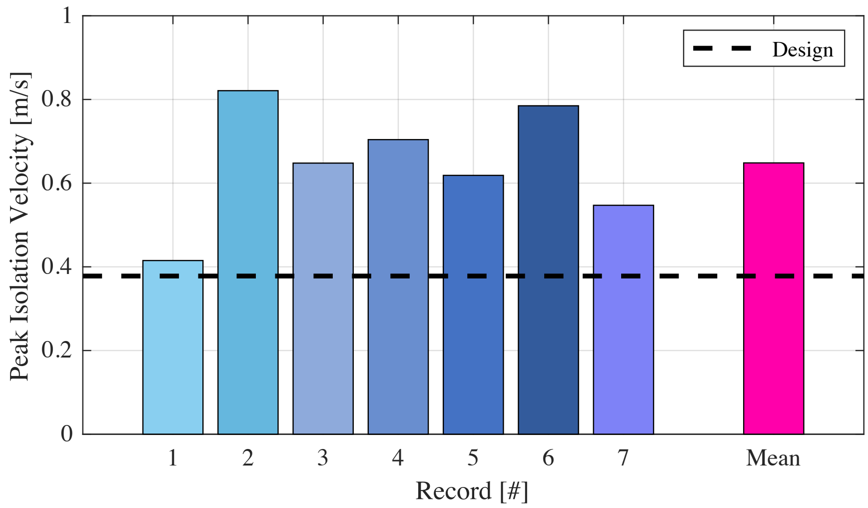

Figure 6: Results: peak isolation velocity.

For what concerns the peak velocity response, it can be noted that NLTHA values are significantly higher, in comparison to the design target value, corresponding to the spectral coordinate of the velocity response spectrum, not only form a single-event standpoint, but also looking to the average response. Variations can be considered within a range bounded between +50% and +100%, with respect to the design target value. Nonetheless, the aforementioned good agreement between the average and the design displacement demands has been found. The main reason of such an aspect can be addressed to the constitutive law for Fluid Viscous Damping deices, which considers a slightly higher damping force, as a consequence of a significant increase of the global velocity.

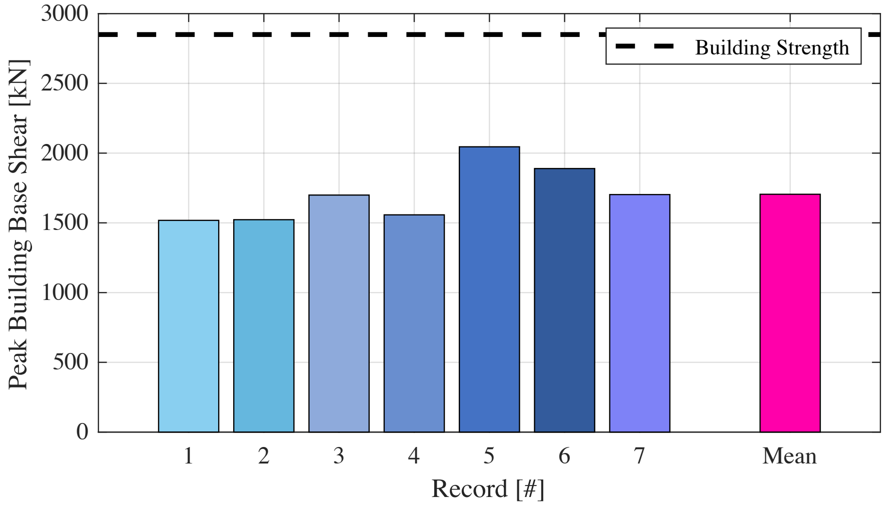

Figure 7: Results: peak building base shear.

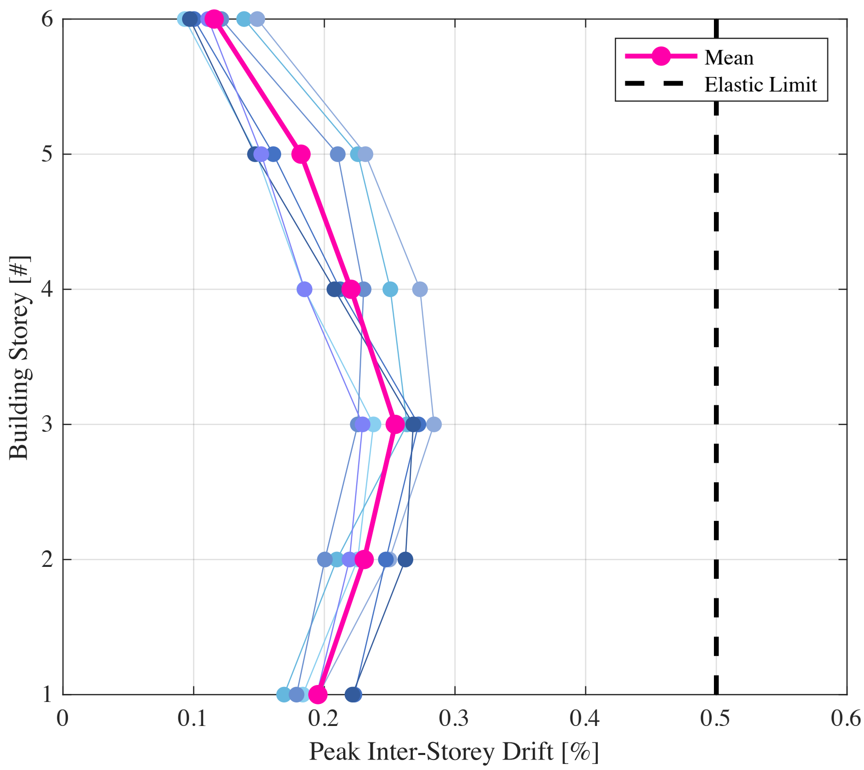

Figure 8: Results: peak inter-storey drift profiles.

Thus, the adopted design procedure leads to a safe evaluation of the target velocity demand of the system, which is consequently underestimated, and then leads to an underdamped solution. Finally results have been analyzed relatively to the effective protection of the superstructure, in terms of base shear and interstorey drift. From both the base shear and interstorey drift responses the superstructure looks significantly protected by the designed isolation system, equipped with fluid viscous dampers, with single-event and average values close to 50% and 60% of the elastic range target values.

6 CONCLUDING REMARKS

In this work a fast design procedure is presented, able to return geometrical and mechanical properties for a seismic isolation system, based on rubber bearings and fluid viscous dampers. The proposed procedure has also been validated, by considering a case study structure, which has been analyzed though NLTHA.
Results have shown the followings:

- The proper design of fluid viscous damping devices allows to consider all bearing points equipped with rubber bearings, and no flat sliders have to be adopted;
- The combination of elastomeric bearings and fluid viscous dampers leads to performance points which are characterized by higher design period, and significantly increased ranges for the equivalent viscous damping ratio, comparable to highly nonlinear isolation systems;
- Results of NLTHA have shown a very good agreement with respect to both the single event and the average peak displacement response, with a significant protection of the superstructure, in terms of both building base shear and interstorey drift values;
- The peak velocity response returned by NLTHA is significantly higher than the corresponding design value, which is computed as the spectral velocity coordinate, which then represents a safe estimation of the damping conditions of the system.

Results should be further investigated, by considering different values of velocity exponent for design, together with possible issues related to vertical buckling of the elastomeric bearings, installed at the internal bearing points of the system, which are expected to be subjected to the highest values of vertical load.

ACKNOWLEDGMENTS

Part of the current work has been carried out under the financial support Italian Civil Protection, within the framework of ReLUIS project 2024-2026 (WP15, Task 15.1).

REFERENCES

[1] Calvi P.M, Calvi G.M. (2018) Historical development of friction-based seismic isolation sys-tems. Soil Dynamics and Earthquake Engineering 106(2018):14-30.

[2] Cardone D., Conte N., Dall'Asta A, Di Cesare A., Flora A., Lamarucciola F., Micozzi F., Ponzo F.C., Ragni L. (2019), "RINTC_E Project: the Seismic Risk of Existing Italian RC Buildings Retrofitted with Seismic Isolation", COMPDYN 2019, 7th ECCOMAS

Thematic Conference on Computational Methods in Structural Dynamics and Earthquake Engineering, Crete, Greece, 24–26 June 2019.

[3] CEN – Comité Européen de Normalisation TC 340 (2018) "European Code UNI EN 15129:2018 Anti-seismic devices", Brussels.

[4] Constantinou M., Mokha A., Reinhorn A. (1990). Teflon bearings in base isolation II: model-ing. Journal of Structural Engineering, 116:455-474.

[5] Constantinou, M. C., Tsopelas, P., Kasalanati, A., and Wolff, E. (1999). "Property modification factors for seismic isolation bearings." Report No. 99-0012, MCEER.

[6] CSI, "SAP2000 v.21.2.0, Integrated Software for Structural Analysis and Design," Computers and Structures Inc., Berkeley, California.

[7] Dall'Asta A, Leoni G, Micozzi F, Gioiella L and Ragni L (2020) A Resilience and Robust-ness Oriented Design of Base-Isolated Structures: The New Camerino University Research Center. Front. Built Environ. 6:50. doi: 10.3389/fbuil.2020.00050

[8] De Domenico D., Ricciardi G., Benzoni G. (2018). Analytical and finite element investigation on the thermo-mechanical coupled response of friction isolators under bidirectional excitation. Soil Dynamics and Earthquake Engineering, 106, 131-147.

[9] De Luca, A.; Guidi, L.G., 2019, "State of art in the worldwide evolution of base isolation design" Soil Dynamics and Earthquake Engineering, 125, 105722, https://doi.org/10.1016/j.soildyn.2019.105722.

[10] Dolce M., Cardone D., Croatto F. (2005) Frictional behavior of steel-PTFE interfaces for seismic isolation. Bulletin of Earthquake Engineering, 3, 75–99.

[11] Fenz D., Constantinou M.C. (2006). Behaviour of the double concave friction pendulum bearing. Earthquake Engineering And Structural Dynamics, 35,1403–1424.

[12] Furinghetti, Marco. 2022. "Definition and Validation of Fast Design Procedures for Seismic Isolation Systems" Vibration, 5, no. 2: 290-305. https://doi.org/10.3390/vibration5020017

[13] Iervolino I., Galasso C., Cosenza E. (2009). REXEL: computer aided record selection for code-based seismic structural analysis. Bulletin of Earthquake Engineering, DOI: 10.1007/s10518-009-9146-1.

[14] Kumar M., Whittaker A.S., Constantinou M.C. (2015). Characterizing friction in sliding isolation bearings. Earthquake Engineering and Structural Dynamics, 44,1409–1425.

[15] Mazza F., Mazza M. (2017) Sensitivity to modelling and design of curved surface sliding bearings in the nonlinear seismic analysis of base-isolated r.c. framed buildings. Soil Dynamics and Earthquake Engineering, 79, 951-970.

[16] NTC 2018, Norme Tecniche per le Costruzioni, Decreto ministeriale del 17 gennaio 2018, in Italian (Italian Building Code, 2018).